



## King's Research Portal

DOI:

[10.1161/CIRCULATIONAHA.112.126920](https://doi.org/10.1161/CIRCULATIONAHA.112.126920)

*Document Version*

Publisher's PDF, also known as Version of record

[Link to publication record in King's Research Portal](#)

*Citation for published version (APA):*

Lewandowski, A. J., Augustine, D., Lamata de la Orden, P., Davis, E. F., Lazdam, M., Francis, J., McCormick, K., Wilkinson, A., Singhal, A., Lucas, A., Smith, N., Neubauer, S., & Leeson, P. (2013). The Preterm Heart in Adult Life: Cardiovascular Magnetic Resonance Reveals Distinct Differences in Left Ventricular Mass, Geometry and Function. *Circulation (Baltimore)*, 127, 197-206. <https://doi.org/10.1161/CIRCULATIONAHA.112.126920>

### Citing this paper

Please note that where the full-text provided on King's Research Portal is the Author Accepted Manuscript or Post-Print version this may differ from the final Published version. If citing, it is advised that you check and use the publisher's definitive version for pagination, volume/issue, and date of publication details. And where the final published version is provided on the Research Portal, if citing you are again advised to check the publisher's website for any subsequent corrections.

### General rights

Copyright and moral rights for the publications made accessible in the Research Portal are retained by the authors and/or other copyright owners and it is a condition of accessing publications that users recognize and abide by the legal requirements associated with these rights.

- Users may download and print one copy of any publication from the Research Portal for the purpose of private study or research.
- You may not further distribute the material or use it for any profit-making activity or commercial gain
- You may freely distribute the URL identifying the publication in the Research Portal

### Take down policy

If you believe that this document breaches copyright please contact [librarypure@kcl.ac.uk](mailto:librarypure@kcl.ac.uk) providing details, and we will remove access to the work immediately and investigate your claim.

## Preterm Heart in Adult Life Cardiovascular Magnetic Resonance Reveals Distinct Differences in Left Ventricular Mass, Geometry, and Function

Adam J. Lewandowski, BSc (Hons); Daniel Augustine, MRCP; Pablo Lamata, PhD;  
Esther F. Davis, MBBS; Merzaka Lazdam, MRCP; Jane Francis, DCR(R), DNM;  
Kenny McCormick, FRCPCH; Andrew R. Wilkinson, FRCPCH; Atul Singhal, FRCP;  
Alan Lucas, FMedSci; Nic P. Smith, PhD; Stefan Neubauer, MD, FRCP, FACC, FMedSci;  
Paul Leeson, PhD, FRCP

**Background**—Preterm birth leads to an early switch from fetal to postnatal circulation before completion of left ventricular in utero development. In animal studies, this results in an adversely remodeled left ventricle. We determined whether preterm birth is associated with a distinct left ventricular structure and function in humans.

**Methods and Results**—A total of 234 individuals 20 to 39 years of age underwent cardiovascular magnetic resonance. One hundred two had been followed prospectively since preterm birth (gestational age=30.3±2.5 week; birth weight=1.3±0.3 kg), and 132 were born at term to uncomplicated pregnancies. Longitudinal and short-axis cine images were used to quantify left ventricular mass, 3-dimensional geometric variation by creation of a unique computational cardiac atlas, and myocardial function. We then determined whether perinatal factors modify these left ventricular parameters. Individuals born preterm had increased left ventricular mass (66.5±10.9 versus 55.4±11.4 g/m<sup>2</sup>;  $P<0.001$ ) with greater prematurity associated with greater mass ( $r=-0.22$ ,  $P=0.03$ ). Preterm-born individuals had short left ventricles with small internal diameters and a displaced apex. Ejection fraction was preserved ( $P>0.99$ ), but both longitudinal systolic (peak strain, strain rate, and velocity,  $P<0.001$ ) and diastolic (peak strain rate and velocity,  $P<0.001$ ) function and rotational (apical and basal peak systolic rotation rate,  $P=0.05$  and  $P=0.006$ ; net twist angle,  $P=0.02$ ) movement were significantly reduced. A diagnosis of preeclampsia during the pregnancy was associated with further reductions in longitudinal peak systolic strain in the offspring ( $P=0.02$ ,  $n=29$ ).

**Conclusions**—Individuals born preterm have increased left ventricular mass in adult life. Furthermore, they exhibit a unique 3-dimensional left ventricular geometry and significant reductions in systolic and diastolic functional parameters.

**Clinical Trial Registration**—URL: <http://www.clinicaltrials.gov>. Unique identifier: NCT01487824. (*Circulation*. 2013;127:197-206.)

**Key Words:** magnetic resonance imaging ■ preeclampsia ■ premature birth ■ ventricular remodeling

Recent improved survival of infants born prematurely has led to a growing cohort of very preterm infants now entering adulthood.<sup>1</sup> Before birth, such adults were often exposed to a suboptimal intrauterine environment, and after delivery, key developmental stages that would normally occur in utero during the third trimester had to take place under ex utero physiological conditions.<sup>2</sup> Because 10% of births are preterm,

any adverse health impact of this unusual developmental pattern is relevant to a large population of adults.

### Editorial see p 160 Clinical Perspective on p 206

Cardiac development may be particularly affected. Birth is associated with a switch in cardiomyocyte phenotype from a

Received June 26, 2012; accepted November 2, 2012.

From the Oxford Cardiovascular Clinical Research Facility (A.J.L., D.A., E.F.D., M.L., P. Leeson) and Oxford Centre for Clinical Magnetic Resonance Research, Department of Cardiovascular Medicine (A.J.L., D.A., J.F., S.N., P. Leeson), and Department of Computer Science (P. Lamata), University of Oxford, Oxford; Department of Paediatrics, John Radcliffe Hospital, Oxford (K.M., A.R.W.); MRC Childhood Nutrition Research Centre, Institute of Child Health, University College London, London (A.S., A.L.); and Department of Biomedical Engineering, King's College London, London (P. Lamata, N. P. S.), UK.

The online-only Data Supplement is available with this article at <http://circ.ahajournals.org/lookup/suppl/doi:10.1161/CIRCULATIONAHA.112.126920/-/DC1>.

Correspondence to Paul Leeson, PhD, FRCP, Oxford Cardiovascular Clinical Research Facility, Department of Cardiovascular Medicine, University of Oxford, John Radcliffe Hospital, Oxford, UK OX39DU. E-mail [paul.leeson@cardiov.ox.ac.uk](mailto:paul.leeson@cardiov.ox.ac.uk)

© 2012 American Heart Association, Inc.

*Circulation* is available at <http://circ.ahajournals.org>

DOI: 10.1161/CIRCULATIONAHA.112.126920

fetal hyperplastic pattern to neonatal hypertrophic response, and animal models demonstrate that this switch also occurs at the time of preterm delivery.<sup>2,3</sup> These cardiomyocytes, which are still relatively immature during the last trimester, are then exposed to significant flow changes as the low-resistance placental circulation transforms into a high-resistance arterial system.<sup>4</sup> Experimental studies demonstrate that, in this setting, cardiomyocytes undergo accelerated hypertrophy with an increase in interstitial myocardial collagen deposition and that the induced changes are sufficient to remodel the left ventricle.<sup>2,3,5</sup>

Cardiovascular magnetic resonance allows accurate, noninvasive assessment of left ventricular structure and function in humans.<sup>6</sup> Computational atlas formation has also introduced the possibility of capturing 3-dimensional geometric variation within populations to explore risk factor influences.<sup>7,8</sup> We used these techniques to reveal for the first time the impact of preterm birth on left ventricular structure and function in humans. Furthermore, we investigated whether key perinatal factors associated with preterm birth such as maternal preeclampsia, growth restriction, and variation in postnatal weight gain had additional impacts on the left ventricle relevant to adult cardiovascular health.

## Methods

### Study Population

We have prospectively followed up individuals born preterm between 1982 and 1985 since recruitment at birth to randomized feeding regimens.<sup>9</sup> The initial cohort of 926 subjects (birth weight <1850 g)<sup>10,11</sup> underwent subgroup review during childhood and adolescence.<sup>12–14</sup> Two hundred forty had agreed to be contacted again, and 102 subjects, who were between 23 and 28 years of age, were able to attend an appointment in Oxford for detailed cardiovascular phenotyping.<sup>10,11</sup> One hundred two young adults born term to uncomplicated pregnancies with age and sex distributions similar to those of the preterm-born young adults were recruited to undergo identical investigations. An older group (30 term-born individuals a decade older with a similar sex distribution) was also recruited to characterize normal aging-related cardiovascular changes. All data were coded with subject- and study-specific identifications (eg, EVS001) to ensure anonymity and blinded analysis. The study was registered with <http://www.clinicaltrials.gov> (NCT01487824); the protocol and recruitment strategy have previously been reported.<sup>10,11</sup> The study was approved by the relevant ethics committee (Oxfordshire Research Ethics Committee A: 06/Q1604/118), and all participants provided signed informed consent.

### Study Visit

#### *Anthropometry and Lifestyle Questionnaire*

Subjects were assessed in the morning after a 12-hour overnight fast. Height was measured to the nearest centimeter and weight to the nearest 0.2 kg with subjects wearing light clothing through the use of a combined digital height and weight measurement station (Seca, UK). Data on medical history, smoking, parental medical history, and lifestyle were obtained with a validated questionnaire.<sup>15</sup>

#### *Blood Samples*

Blood samples were drawn, centrifuged, and separated within 30 minutes and then stored for later analysis at  $-80^{\circ}\text{C}$ . Fasting blood biochemistry was measured at the Oxford John Radcliffe Hospital Biochemistry Laboratory through the use of routine validated assays with clinical-level quality controls.

#### *Blood Pressure*

Three brachial blood pressure measurements were recorded on the left arm with an automatic digital monitor (HEM-705CP; OMRON,

Japan), and the second and third measurements were averaged for analysis.<sup>9–11</sup> Aortic blood pressure was assessed by left radial artery applanation tonometry to derive ascending aortic pressure waveforms (SphygmoCor Analysis System, Australia).

### *Cardiovascular Magnetic Resonance*

Cardiovascular magnetic resonance was performed on a 1.5-T Siemens Sonata scanner. Steady-state free-precession cine sequences were used to acquire localization images, followed by optimized left ventricular horizontal and vertical long-axis cines. From these, a left ventricular short-axis cine stack was obtained with standardized basal slice alignment with a 7-mm slice thickness and 3-mm interslice gap. All cardiovascular magnetic resonance imaging was prospectively ECG gated with a precordial 3-lead ECG and acquired during end-expiration breath holding. Image acquisition parameters for the steady-state free-precession images were as follows: echo time, 1.5 milliseconds; repetition time, 3.0 milliseconds; and flip angle,  $60^{\circ}$ . The short- and long-axis steady-state free-precession images were stored on a digital archive for postprocessing, which was undertaken as detailed below.

### Quantification of Left Ventricular Mass

Image analysis for left ventricular volumes and mass was performed offline on the short-axis cine stack with Siemens analytic software (Argus, Siemens Medical Solutions, Germany). Left ventricular short-axis epicardial and endocardial borders were manually contoured at end diastole and end systole to allow automated calculation of left ventricular mass and volumes. Mass represents the following:  $(\text{end-diastolic epicardial} - \text{endocardial volume}) \times 1.05$ . Stroke volume is end-diastolic volume minus end-systolic volume, and ejection fraction is given by the following:  $(\text{stroke volume} / \text{end-diastolic volume}) \times 100\%$ . Wall thickness was measured on the midventricular short-axis slice at end diastole, and internal and external cavity diameters were measured on the midventricular short-axis slice at end diastole between the septum and inferolateral wall. Ventricular length was measured at end diastole on the horizontal long-axis cine between the left ventricular apex and middle of the mitral annulus. Relative wall thickness was calculated as follows:  $(2 \times \text{inferior wall thickness}) / \text{end-diastolic diameter}$ .

### Creation of Cardiac Atlas for Assessment of Left Ventricular Geometry

Creation of a cardiac statistical atlas of all cardiovascular magnetic resonance images was undertaken in collaboration with the Department of Computer Science, University of Oxford and Department of Biomedical Engineering, King's College London using recently published methods.<sup>8</sup> The end-diastolic frame from the DICOM (digital imaging and communications in medicine) file for each slice of the left ventricular short-axis cine stack that included the manually contoured endocardial and epicardial contours drawn with Argus was retrieved and rebuilt into a single DICOM file with MatLab R2011b (The Mathworks, Natick, MA). The file was converted into a binary segmentation image representing the left ventricle, and a mesh was fitted to this myocardial anatomy, achieving subvoxel accuracy (average fitting error, 1.24 mm).<sup>8</sup> The left ventricular anatomy of each subject was then described with a mesh defined by a set of 3456 nodal variables (or degrees of freedom). Principal component analysis was undertaken to identify the key modes of variation of the shape, reducing the parametric space for comparisons from 3456 to 6 dimensions. The left ventricular meshes for the population have been made available to the scientific community ([amdb.isd.kcl.ac.uk](http://amdb.isd.kcl.ac.uk)).<sup>16</sup>

### Assessment of Left Ventricular Systolic and Diastolic Function

In addition to gross volumetric measures of systolic left ventricular function (ejection fraction and stroke volume), we evaluated both systolic and diastolic function, including cardiac rotational

movement, on the basis of myocardial deformation parameters assessed with TomTec 2D Cardiac Performance Analysis MR (TomTec Diogenes, Germany). The endocardial borders of the left ventricular steady-state free-precession horizontal long-axis cine and basal, mid, and apical left ventricular short-axis cines were manually contoured on the end-diastolic frame. The software then tracked the motion of related features adjacent to this endocardial line such as the cavity-tissue boundary or individual tissue patterns over the cardiac cycle to produce endocardial strain parameters.<sup>17</sup> The averages of segmental strains from the short-axis planes were used for endocardial circumferential strain, and the average of segmental strain in the horizontal long-axis view was used for global endocardial longitudinal strain. Net twist angle was calculated as peak apical endocardial circumferential rotation minus peak basal endocardial circumferential rotation.

### Statistical Analysis

Statistical analysis was carried out with SPSS version 19. Normality of variables was assessed by visual assessment of normality curves and the Shapiro-Wilk test. Comparison between groups for continuous variables was performed with a 2-sided, independent-samples Student *t* test for normally distributed data and Mann-Whitney and Kruskal-Wallis tests for skewed data. For categorical variables, comparison was done with a  $\chi^2$  test. Linear regression models were performed with a forced entry method. Pearson correlations (*r*) were used for bivariate associations, and unstandardized regression coefficients (B) were used for bivariate and multivariate regression models. Analysis was repeated with and without inclusion of 6 sets of preterm-born twins, but because no differences were observed, results are presented with twins included in the preterm-born cohort. Having 102 subjects per group provided us with 80% power at  $P=0.05$  to identify a 0.38-SD difference between groups, equivalent to a 10-g difference in left ventricular mass, and a 0.58-SD difference between each young adult group and the older adults. Results are presented as mean $\pm$ SD. When multiple comparisons were performed between groups, *P* values were adjusted with the Bonferroni method. Comparisons between preterm-born young adults and term-born young adults were adjusted for age and sex, whereas comparisons between preterm-born and term-born young adults and the older term-born older adults were adjusted for sex. Values of  $P < 0.05$  were considered statistically significant.

## Results

### Study Population Characteristics

Compared with the original cohort of preterm-born individuals recruited at birth, those followed up in young adulthood were similar in perinatal characteristics (Table I in the online-only Data Supplement) except for a small 70-g (5%) difference in birth weight. This is accounted for by a marginally more preterm cohort so that birth weight Z score is identical between groups. Of the 102 individuals in the cohort, 14 (13.7%) were born extremely preterm (<28 weeks), 56 (54.9%) were born very preterm (28–31 weeks), and 32 (31.4%) were born moderate to late preterm (32–36 weeks). In adult life, there were no significant differences in number of smokers, personal and family medical histories, or lifestyle factors such as socioeconomic status, physical activity, or diet (results not shown). Adults born preterm were shorter and weighed more than the young adult term-born cohort (Table 1) and had a distinct metabolic profile. Total and low-density lipoprotein cholesterol, triglyceride, glucose, and insulin levels were significantly increased (Table II in the online-only Data Supplement). Brachial and aortic blood pressure parameters were also elevated compared with the term-born cohort of similar age, with levels similar to those in individuals a decade older (Table II in the online-only Data Supplement).

### Elevated Left Ventricular Mass in Preterm-Born Young Adults

Those born preterm had a 19-g higher left ventricular mass and significantly increased mass indexed to body surface area compared with term-born young adults (left ventricular mass, 121.1 $\pm$ 27.3 versus 102.1 $\pm$ 26.8 g,  $P < 0.001$ ; mass index, 66.5 $\pm$ 10.9 versus 55.4 $\pm$ 11.4 g/m<sup>2</sup>,  $P < 0.001$ ; Figure 1A). Within the preterm group, the more premature their birth was, the greater their left ventricular mass in young adult life was ( $r = -0.22$ ,  $P = 0.03$ ).

**Table 1. Characteristics of Cohorts**

|                        | Preterm-Born Young Adults (n=102) | Term-Born Young Adults (n=102) | <i>P</i> * | Term-Born Adults (n=30) | <i>P</i> † | <i>P</i> ‡ |
|------------------------|-----------------------------------|--------------------------------|------------|-------------------------|------------|------------|
| <b>Demographics</b>    |                                   |                                |            |                         |            |            |
| Gestational age, wk    | 30.3 $\pm$ 2.5                    | 39.6 $\pm$ 0.9                 |            | 39.8 $\pm$ 0.8          |            |            |
| Age, y                 | 25.1 $\pm$ 1.4                    | 25.0 $\pm$ 2.6                 |            | 35.5 $\pm$ 1.8          |            |            |
| Males, n (%)           | 47 (46.1)                         | 47 (46.1)                      |            | 14 (46.7)               |            |            |
| Smokers, n (%)         | 20 (19.6)                         | 20 (19.6)                      | >0.99      | 3 (10.0)                | 0.63       | 0.63       |
| <b>Anthropometrics</b> |                                   |                                |            |                         |            |            |
| Birth weight, g        | 1297.0 $\pm$ 286.8                | 3460.0 $\pm$ 417.0             |            | 3301.9 $\pm$ 423.9      |            |            |
| Height, cm             | 169.1 $\pm$ 10.0                  | 173.5 $\pm$ 9.0                | <0.001     | 169.3 $\pm$ 9.6         | >0.99      | 0.01       |
| Weight, kg             | 73.0 $\pm$ 20.5                   | 69.3 $\pm$ 12.5                | 0.33       | 79.8 $\pm$ 28.9         | 0.46       | 0.01       |
| BMI, kg/m <sup>2</sup> | 24.9 $\pm$ 5.4                    | 22.9 $\pm$ 3.1                 | 0.003      | 27.1 $\pm$ 9.6          | 0.33       | <0.001     |
| BSA, m <sup>2</sup>    | 1.81 $\pm$ 0.21                   | 1.83 $\pm$ 0.20                | >0.99      | 1.84 $\pm$ 0.21         | >0.99      | >0.99      |
| Waist/hip ratio        | 0.78 $\pm$ 0.10                   | 0.81 $\pm$ 0.06                | 0.91       | 0.81 $\pm$ 0.08         | >0.99      | >0.99      |

Values as are given as mean $\pm$ SD unless stated otherwise. *P* values were adjusted with the Bonferroni method.

\*Preterm-born young adults versus term-born young adults. Comparisons adjusted for age and sex.

†Preterm-born young adults versus term-born adults. Comparisons adjusted for sex.

‡Term-born young adults versus term-born adults. Comparisons adjusted for sex.



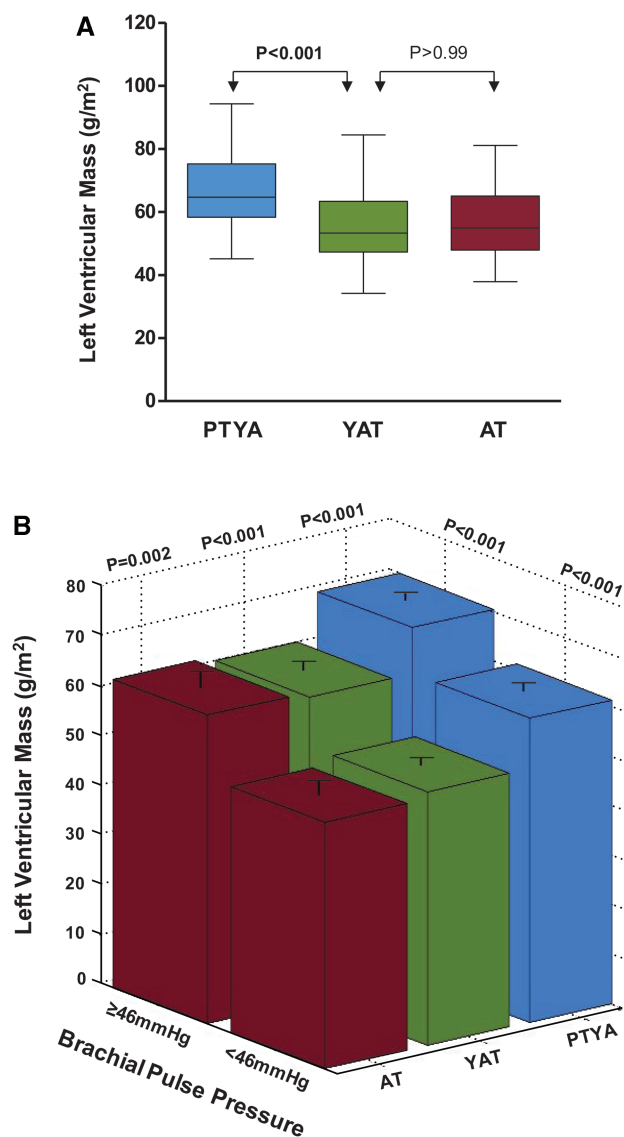


**Figure 1. A**, Left ventricular mass indexed to body surface area (LVMI). LVMI was higher in preterm-born young adults (PTYAs; blue;  $66.5 \pm 10.9$  g/m<sup>2</sup>) than young adults born at term (YATs; green;  $55.4 \pm 11.4$  g/m<sup>2</sup>;  $P < 0.001$ ) and adults a decade older born at term (ATs; red;  $51.1 \pm 10.7$  g/m<sup>2</sup>;  $P < 0.001$ ). LVMI of the ATs did not differ from that of the YATs ( $P > 0.99$ ). **B**, Comparison of LVMI by equivalent blood pressure groups. The median brachial pulse pressure (46 mmHg) for the entire population was used as a cut-off point to divide each subgroup (PTYAs, blue; YATs, green; ATs, red) into 2 groups. Comparison of those with brachial pulse pressure  $< 46$  mmHg ( $n = 44$  PTYAs,  $n = 58$  YATs, and  $n = 13$  ATs) showed that PTYAs had significantly higher LVMI compared with YATs and ATs ( $61.2 \pm 9.8$  vs  $51.1 \pm 10.7$  g/m<sup>2</sup> [ $P < 0.001$ ] vs  $49.6 \pm 10.3$  g/m<sup>2</sup> [ $P < 0.001$ ]). Comparison of those with brachial pulse pressure  $\geq 46$  mmHg ( $n = 58$  PTYAs,  $n = 44$  YATs, and  $n = 17$  ATs) showed that PTYAs had a magnitude of elevation of LVMI similar to that of both YATs and ATs ( $70.5 \pm 10.0$  vs  $61.2 \pm 9.8$  g/m<sup>2</sup> [ $P < 0.001$ ] vs  $62.1 \pm 10.4$  g/m<sup>2</sup> [ $P = 0.003$ ]).

Blood pressure was associated with left ventricular mass in all study groups, with brachial pulse pressure the most closely related parameter in the preterm-born ( $r = 0.54$ ,  $P < 0.001$ ), term-born ( $r = 0.54$ ,  $P < 0.001$ ), and older ( $r = 0.68$ ,  $P < 0.001$ ) adults. Therefore, because blood pressure in young adulthood was higher in those born preterm, we explored to what extent

this accounted for their higher left ventricular mass. Initially, because the older term-born adults had blood pressure levels similar to those of the preterm group, we compared levels of left ventricular mass between these groups and found that mass and mass index were significantly higher in the younger preterm-born adults ( $P < 0.001$  and  $P < 0.001$ ; Figure 1A), consistent with an impact of prematurity on left ventricular mass that was independent of absolute blood pressure levels alone. To ensure that the variation in age between these groups did not confound the comparison, we also carried out a complementary analysis based on a comparison of the impact of prematurity with the study participants stratified into high- and low-blood-pressure groups around the median brachial pulse pressure within the cohort (Figure 1B). Left ventricular mass was higher in those in the higher-blood-pressure group, consistent with an impact of blood pressure on left ventricular mass. However, those born preterm had additional significant increases in mass index, regardless of blood pressure level, compared with both the term-born young adults and the older adults ( $61.2 \pm 9.8$  versus  $51.1 \pm 10.7$  g/m<sup>2</sup> [ $P < 0.001$ ] versus  $49.6 \pm 10.3$  g/m<sup>2</sup> [ $P < 0.001$ ] in those with pulse pressure  $< 46$  mmHg and  $70.5 \pm 10.0$  versus  $61.2 \pm 9.8$  g/m<sup>2</sup> [ $P < 0.001$ ] versus  $62.1 \pm 10.4$  g/m<sup>2</sup> [ $P = 0.003$ ] in those with a pulse pressure  $\geq 46$  mmHg).

Finally, we used a linear regression model to take into account other potential factors related to left ventricular mass within the preterm-born and term-born young adult groups. Within sets of interrelated variables such as blood pressure, the variable with the strongest correlation was included, leaving 6 independent variables significantly related to mass index ( $P < 0.05$ ; Table III in the online-only Data Supplement) to be included in the model (glucose level, high-density lipoprotein cholesterol, waist-to-hip ratio, sex, brachial pulse pressure, and premature birth as dichotomous categorical variables, with young adults born at term as 1 and those at preterm as 2). In this model, prematurity remained an independent predictor of mass index ( $B = 10.23$  g/m<sup>2</sup> per group;  $P < 0.001$ ; 95% confidence interval, 7.48–12.98).

### Geometric Changes in the Preterm Left Ventricle

We then studied variation in left ventricular geometry. Principal component analysis was used to identify the major modes of variation within the 3-dimensional meshes generated from each of the cardiac data sets. All identified modes were numbered in order on the basis of the amount of variation within the population each accounted for (with mode 1 accounting for the greatest proportion, 29.8%). When we compared the preterm cohort with the term-born individuals of similar age, we observed significant differences between groups in the first 6 modes, with levels of significance for modes 1, 2, and 5 being in the order  $P = 1 \times 10^{-11}$  to  $P = 1 \times 10^{-13}$  (Figure 2A). These first 6 modes accounted for 84.2% of the variance in left ventricular geometry within the study population (Figure 2B). Four of these modes also reached significance for differences between the preterm group and the older term-born adults, but no modes reached significance when the 2 term-born cohorts were compared (Figure 2A). Figure 2C demonstrates where the mean of each group lies relative to the other groups in the principal component analysis parametric space. Separation between

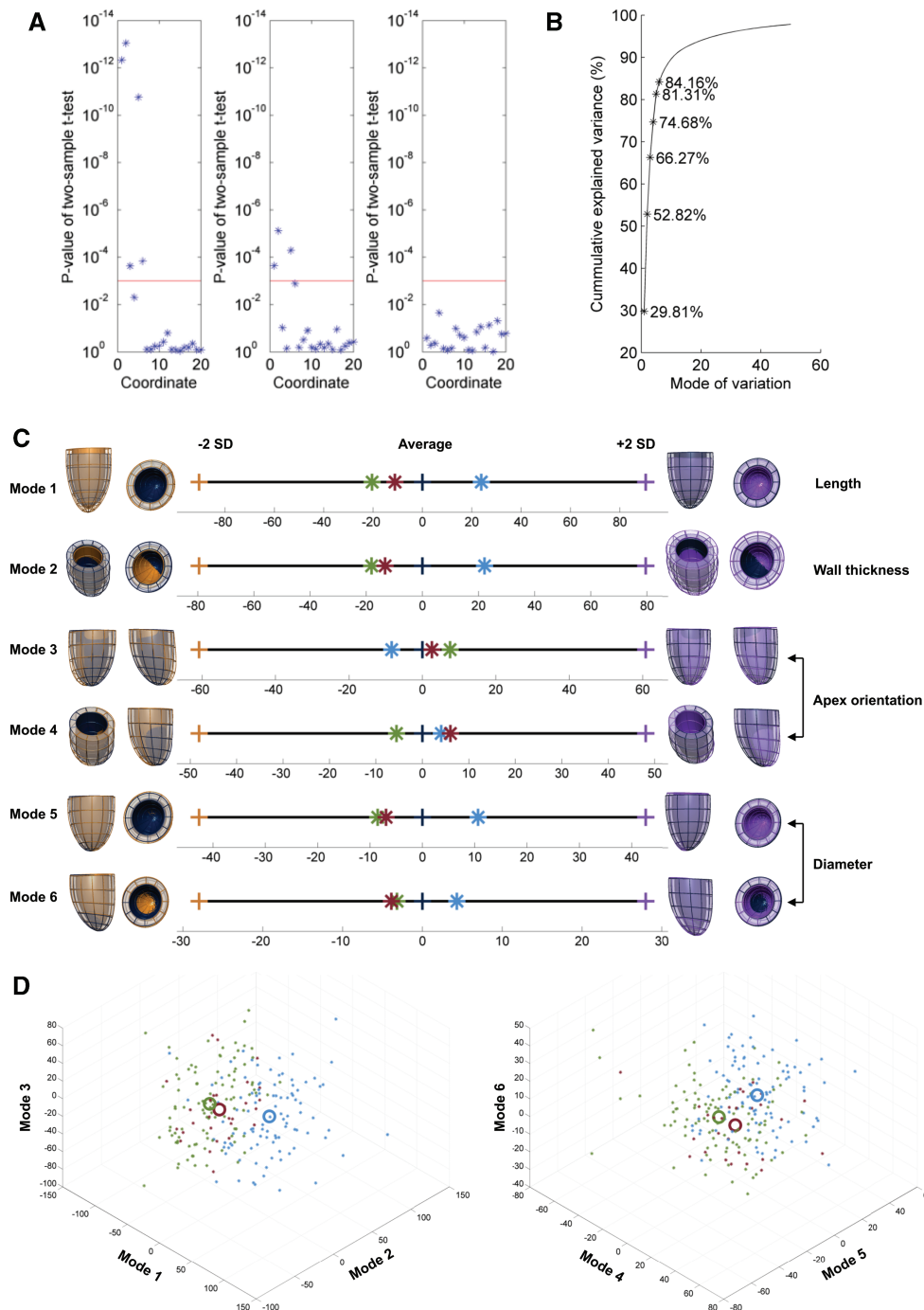


**Figure 2.** **A**, Comparison of differences in shape between groups by modes of variation of the principal component analysis (PCA). Comparison between groups was performed with a 2-sided Student *t* test. The red line indicates  $P=0.01$ . Left, A comparison of the preterm-born young adults (PTYAs) and young adults born at term (YATs) demonstrating that the first 6 modes of variation differed significantly between groups. Middle, A comparison of the PTYAs and older adult term-born (AT) groups demonstrating that modes 1, 2, 5, and 6 were significantly different between groups. Right, A comparison of the YAT and AT groups demonstrating no significant differences between groups. **B**, Cumulative variance explained by each mode of variation. The first 6 modes of variation, which differed between the PTYA and YAT groups (see **C**), explained 84.2% of the variance in left ventricular (LV) geometry within the entire population, with mode 1 explaining the majority of variance (29.8%). **C**, The first 6 independent modes of variation resulting from the PCA. In all 6 cases, the average is at coordinate 0 and is represented by a dark blue cross and the dark blue LV mesh overlaid on the orange and purple meshes. The orange cross and orange LV mesh represent  $-2$  SD for each mode of variation; the purple cross and purple LV mesh,  $2$  SD for each mode of variation. As illustrated here, the modes of variation represent changes in the following: 1=primarily ventricular length with a proportion of diameter change; 2=wall thickness; 3 and 4=apex orientation; 5=primarily diameter with a proportion of apex position; and 6=primarily diameter with a proportion of length change. The stars represent the PCA coordinates for the average for each group (PTYAs, blue; YATs, green; ATs, red) for each mode of variation. **D**, Distribution of all subjects in the PCA coordinates. Averages for the group are indicated by a circle. Left, The first 3 modes of variation (1–3); right, the next 3 modes of variation (4–6).

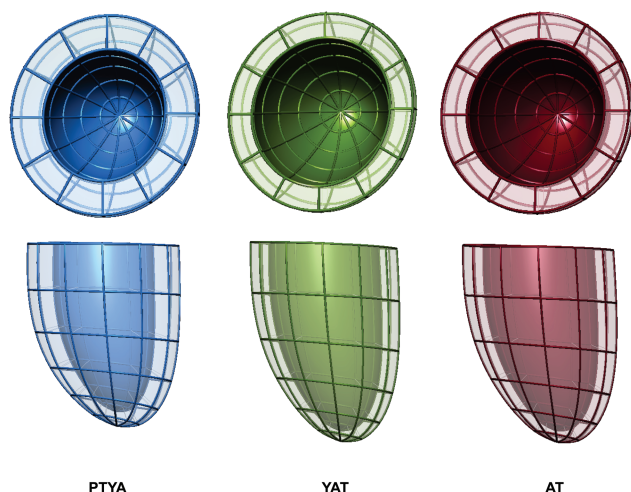


**Figure 3.** Statistical average shape for each group. AT indicates older term-born adults (red); PTYA, preterm-born young adults (blue); and YAT, term-born young adults (green).

preterm and term-born offspring is also evident when individual subject data are plotted in 3 dimensions (Figure 2D).

We visually assessed models that corresponded with  $\pm 2$  SD of the mean variation for the 6 modes that differed between preterm and term-born individuals. The geometric differences each describes are shown in Figure 2C. Preterm-born individuals had significantly shorter ventricles, increased left ventricular wall thickness, a shift in apex orientation away from the right ventricle, and reduced internal left ventricular cavity diameter (Figure 2C and Figure 3). Several of these features could be captured by standard clinical left ventricular measures, specifically left ventricular length, cavity diameters, and wall thickness at end diastole. We confirmed differences in

these standard measures between preterm-born young adults and term-born individuals (Table 2). In view of the combination of increased wall thickness and reduced ventricular cavity size, we also calculated relative wall thickness and left ventricular mass relative to end-diastolic volume (left ventricular mass/end-diastolic volume; Table 2). Twenty-one individuals born preterm (20.6%) had a relative wall thickness  $>0.42$  compared with none in either term-born group. Furthermore, those born preterm had increased left ventricular mass/end-diastolic volume compared with both term-born groups ( $P<0.001$ ; Table 2), with an inverse association between gestational age and left ventricular mass/end-diastolic volume ( $r=-0.36$ ,  $P<0.001$ ).

### Altered Left Ventricular Systolic and Diastolic Function

We then evaluated whether there were also changes in left ventricular function related to prematurity. End-systolic volume was reduced and stroke volume was smaller in the preterm group, with the reduction graded according to the degree of prematurity ( $r=-0.20$ ,  $P=0.05$ ). Although ejection fraction did not differ, myocardial deformation patterns were significantly altered in those born preterm (Table 3). Longitudinal peak systolic strain and peak systolic strain rate were reduced compared with both term-born groups (Figure 4A and 4B). Furthermore, systolic rotational behavior varied with reduced basal and apical rotation rates (Table 3). Diastolic myocardial relaxation was also reduced with slower longitudinal peak diastolic strain rates compared with term-born individuals of similar age. Interestingly, longitudinal peak diastolic strain rates were reduced in the older adults to a degree similar to that measured in those born preterm (Figure 4A and 4B).

**Table 2. Left Ventricular Volumes and Dimensions**

|  | Preterm-Born Young Adults<br>(n=102) | Term-Born Young Adults<br>(n=102) | <i>P</i> * | Term-Born Adults<br>(n=30) | <i>P</i> † | <i>P</i> ‡ |
|--|--------------------------------------|-----------------------------------|------------|----------------------------|------------|------------|
| ED volume, mL/m <sup>2</sup>           | 72.2±9.3                             | 80.2±11.7                         | <0.001     | 81.5±12.9                  | <0.001     | >0.99      |
| End-systolic volume, mL/m <sup>2</sup> | 25.7±5.4                             | 29.1±6.4                          | <0.001     | 29.0±6.4                   | 0.01       | >0.99      |
| Stroke volume, mL/m <sup>2</sup>       | 46.6±7.4                             | 51.3±8.9                          | <0.001     | 52.5±8.4                   | <0.001     | >0.99      |
| Length, cm                             | 9.20±0.65                            | 9.81±0.73                         | <0.001     | 9.70±0.64                  | <0.001     | >0.99      |
| Luminal diameter, cm                   | 5.20±0.47                            | 5.64±0.48                         | <0.001     | 5.66±0.34                  | <0.001     | >0.99      |
| External diameter, cm                  | 7.33±0.65                            | 7.19±0.64                         | 0.16       | 7.26±0.43                  | >0.99      | >0.99      |
| Global ED WT, mm                       | 9.26±1.40                            | 7.46±1.26                         | <0.001     | 7.93±1.26                  | <0.001     | 0.07       |
| Anterior ED WT, mm                     | 8.21±1.51                            | 6.87±1.51                         | <0.001     | 7.39±1.45                  | 0.009      | 0.15       |
| Anterolateral ED WT, mm                | 8.89±1.74                            | 6.89±1.45                         | <0.001     | 7.11±1.50                  | <0.001     | >0.99      |
| Inferolateral ED WT, mm                | 9.40±1.75                            | 7.13±1.53                         | <0.001     | 7.52±1.38                  | <0.001     | 0.44       |
| Inferior ED WT, mm                     | 9.17±1.73                            | 7.22±1.60                         | <0.001     | 8.03±1.45                  | 0.003      | 0.01       |
| Inferoseptal ED WT, mm                 | 10.29±1.80                           | 8.56±1.34                         | <0.001     | 8.96±1.58                  | <0.001     | 0.40       |
| Anteroseptal ED WT, mm                 | 9.63±1.79                            | 8.10±1.78                         | <0.001     | 8.56±1.68                  | 0.003      | 0.51       |
| Relative WT                            | 0.35±0.07                            | 0.26±0.05                         | <0.001     | 0.28±0.05                  | <0.001     | 0.02       |
| Relative WT >0.42, n (%)               | 21 (20.6)                            | 0 (0)                             | <0.001     | 0 (0)                      | <0.001     | >0.99      |
| Mass/ED volume, g/mL                   | 0.93±0.14                            | 0.70±0.12                         | <0.001     | 0.70±0.13                  | <0.001     | >0.99      |

ED indicates end-diastolic; WT, wall thickness. Values as mean±SD unless stated otherwise. *P* values were adjusted with the Bonferroni method.

\*Preterm-born young adults versus term-born young adults. Comparisons adjusted for age and sex.

†Preterm-born young adults versus term-born adults. Comparisons adjusted for sex.

‡Term-born young adults versus term-born adults. Comparisons adjusted for sex.

**Table 3. Left Ventricular Systolic and Diastolic Function**

|                           | Preterm-Born Young Adults<br>(n=102) | Term-Born Young Adults<br>(n=102) | <i>P</i> <sup>*</sup> | Term-Born Adults (n=30) | <i>P</i> <sup>†</sup> | <i>P</i> <sup>‡</sup> |
|---------------------------|--------------------------------------|-----------------------------------|-----------------------|-------------------------|-----------------------|-----------------------|
| <b>Systolic function</b>  |                                      |                                   |                       |                         |                       |                       |
| Ejection fraction, %      | 64.5±6.1                             | 64.1±4.9                          | >0.99                 | 64.3±4.8                | >0.99                 | >0.99                 |
| <b>Longitudinal</b>       |                                      |                                   |                       |                         |                       |                       |
| Strain, %                 | -14.8±3.2                            | -17.9±4.1                         | <0.001                | -17.7±5.3               | 0.003                 | >0.99                 |
| Strain rate, %/s          | -0.90±0.21                           | -1.06±0.31                        | <0.001                | -1.08±0.31              | 0.009                 | >0.99                 |
| Displacement, cm          | 3.80±1.47                            | 4.71±2.54                         | 0.01                  | 4.23±1.56               | 0.68                  | >0.99                 |
| Velocity, cm/s            | 2.25±0.78                            | 3.09±0.97                         | <0.001                | 3.17±1.18               | <0.001                | >0.99                 |
| <b>Circumferential</b>    |                                      |                                   |                       |                         |                       |                       |
| Basal strain, %           | -21.2±2.9                            | -21.8±3.2                         | 0.45                  | -22.2±3.4               | 0.38                  | >0.99                 |
| Basal strain rate, %/s    | -1.26±0.21                           | -1.28±0.24                        | >0.99                 | -1.32±0.28              | 0.63                  | >0.99                 |
| Basal rotation, °         | -7.21±4.59                           | -8.81±5.22                        | 0.08                  | -7.65±4.12              | >0.99                 | 0.88                  |
| Basal rotation rate, °/s  | -46.2±26.4                           | -60.2±35.4                        | 0.006                 | -52.1±29.2              | >0.99                 | 0.83                  |
| Mid strain, %             | -17.9±2.2                            | -17.7±2.2                         | >0.99                 | -18.3±2.2               | >0.99                 | 0.61                  |
| Mid strain rate, %/s      | -1.06±0.14                           | -1.04±0.19                        | >0.99                 | -1.09±0.18              | >0.99                 | 0.97                  |
| Apical strain, %          | -21.6±3.8                            | -22.1±3.8                         | >0.99                 | -22.8±4.0               | 0.45                  | >0.99                 |
| Apical strain rate, %/s   | -1.30±0.24                           | -1.25±0.24                        | 0.39                  | -1.33±0.24              | >0.99                 | 0.40                  |
| Apical rotation, °        | 7.04±4.35                            | 7.95±5.54                         | 0.63                  | 6.13±4.66               | >0.99                 | 0.42                  |
| Apical rotation rate, °/s | 46.3±26.2                            | 56.1±30.1                         | 0.05                  | 42.0±22.8               | >0.99                 | 0.04                  |
| Net twist angle, °        | 14.0±6.4                             | 16.9±7.8                          | 0.02                  | 13.5±6.3                | >0.99                 | 0.18                  |
| <b>Diastolic function</b> |                                      |                                   |                       |                         |                       |                       |
| <b>Longitudinal</b>       |                                      |                                   |                       |                         |                       |                       |
| Strain rate, %/s          | 0.95±0.35                            | 1.31±0.52                         | <0.001                | 1.07±0.31               | 0.41                  | 0.01                  |
| Velocity, cm/s            | -2.38±0.81                           | -3.22±1.36                        | <0.001                | -2.60±1.14              | 0.84                  | 0.09                  |
| <b>Circumferential</b>    |                                      |                                   |                       |                         |                       |                       |
| Basal strain rate, %/s    | 1.42±0.24                            | 1.62±0.39                         | <0.001                | 1.55±0.42               | 0.11                  | >0.99                 |
| Basal rotation rate, °/s  | 56.7±37.5                            | 71.4±40.5                         | 0.03                  | 73.3±45.7               | 0.16                  | >0.99                 |
| Mid strain rate, %/s      | 1.13±0.18                            | 1.13±0.19                         | >0.99                 | 1.18±0.21               | 0.59                  | 0.67                  |
| Apical strain rate, %/s   | 1.45±0.36                            | 1.44±0.39                         | >0.99                 | 1.42±0.34               | >0.99                 | >0.99                 |
| Apical rotation rate, °/s | -45.5±27.7                           | -52.3±41.8                        | 0.57                  | -48.0±35.3              | >0.99                 | >0.99                 |

Values as mean±SD unless stated otherwise. *P* values were adjusted with the Bonferroni method.

\*Preterm-born young adults versus term-born young adults. Comparisons adjusted for age and sex.

†Preterm-born young adults versus term-born adults. Comparisons adjusted for sex.

‡Term-born young adults versus term-born adults. Comparisons adjusted for sex.

### Preterm Birth Risk Factors and Left Ventricular Geometry and Function

To understand whether prematurity per se or factors linked with prematurity accounted for the variation in the key geometric (left ventricular mass index, length, and end-diastolic volume) and functional (longitudinal peak systolic strain, peak systolic strain rate and diastolic strain rate) variables that differed in those born preterm, we performed further regression analyses. For each outcome variable, we performed 2 regression models. Because our sample size was 102 individuals, we limited the number of variables included to 5 key perinatal characteristics (gestational age, birth weight Z score, postnatal weight gain in the first 2 weeks, days of ventilation, and maternal preeclampsia). Those characteristics that were significant in this model were included in a second model that incorporated potentially relevant cardiovascular risk factors in young adulthood (high-density lipoprotein, sex, waist-to-hip ratio, glucose, and brachial pulse pressure).

Gestational age was associated with left ventricular structure in this preterm group (Table IV in the online-only Data Supplement). For left ventricular mass index, gestational age was the only independent predictor in model 1 (*P*=0.02) and remained an independent predictor in model 2 (*P*=0.03). For left ventricular length, gestational age and birth weight Z score were both independent predictors in model 1 (*P*=0.03 and *P*=0.04), but only gestational age remained significant in model 2 (*P*=0.02 and *P*=0.11). For end-diastolic volume, gestational age approached significance in model 1 (*P*=0.08) and was significant in model 2 (*P*=0.05).

Interestingly, when we modeled functional variables, maternal preeclampsia, but not other variables, accounted for a proportion of variation in longitudinal peak systolic strain within the preterm group in model 1 (*P*=0.05) and remained significant in model 2 (*P*=0.05). Nearly a third (*n*=29) of our preterm group were born to a pregnancy complicated by preeclampsia. The absolute global peak longitudinal systolic strain in those



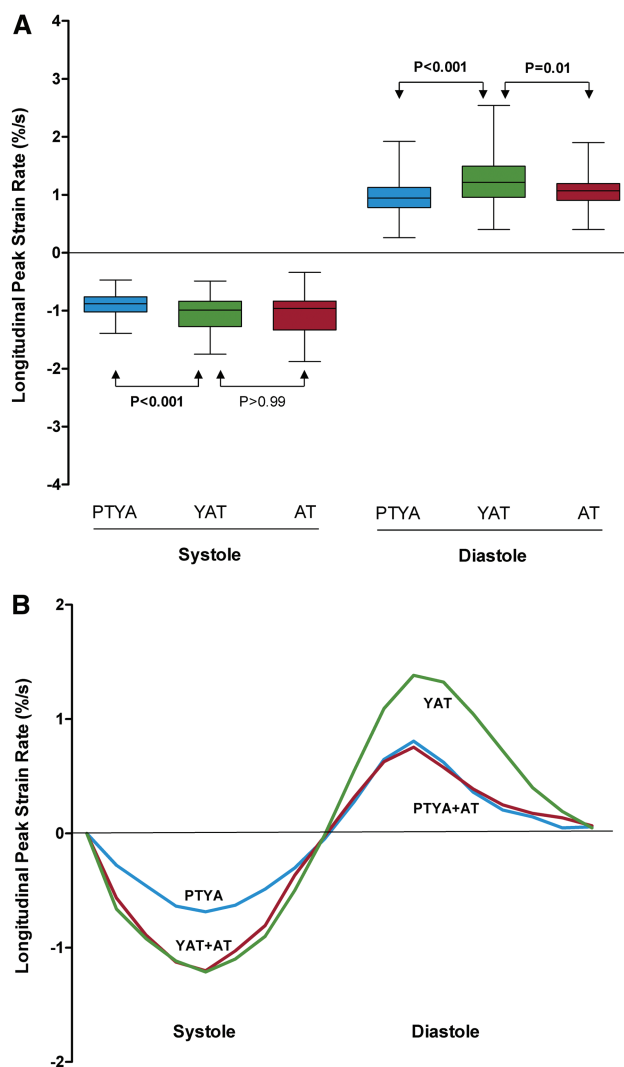


**Figure 4.** **A**, Longitudinal peak systolic and diastolic strain rates. Preterm-term born young adults (PTYAs; blue) have reduced longitudinal peak systolic strain rate ( $-0.90 \pm 0.21$ /s) compared with both the young adults born term (YATs; green;  $-1.06 \pm 0.31$ /s;  $P < 0.001$ ) and the older term-born adults (ATs; red;  $-1.08 \pm 0.31$ /s;  $P = 0.003$ ). However, although longitudinal peak diastolic strain rate in the PTYAs was still reduced compared with the YATs ( $0.95 \pm 0.35$ /s vs  $1.31 \pm 0.52$ /s;  $P < 0.001$ ), it did not differ from the ATs ( $1.07 \pm 0.31$ /s;  $P = 0.41$ ). **B**, Example longitudinal strain rate curves for each group. YATs and ATs showed similar longitudinal strain rates in systole, which differed from the PTYAs. In diastole, longitudinal strain rates were similar for the PTYAs and ATs, which differed from the YATs.

born preterm to a preeclamptic pregnancy was  $-13.8 \pm 2.2\%$  compared with  $-15.2 \pm 3.4\%$  in those born preterm to normotensive mothers ( $P = 0.02$ ). This appeared to be additional to any impact of prematurity on longitudinal peak systolic strain because individuals born preterm to normotensive pregnancies still showed a significant reduction in longitudinal peak systolic strain compared with term-born individuals of similar age ( $P < 0.001$ ).

## Discussion

This study demonstrates for the first time that young adults born preterm have a unique adverse left ventricular structure and function. Left ventricular mass is significantly increased and the

left ventricles are shorter with reduced cardiac volumes and apical displacement. Furthermore, prematurity is associated with reductions in systolic, diastolic, and rotational function. The variation in structure appears to be determined by preterm birth, with the severity of changes graded according to the degree of prematurity, not by any specific associated perinatal exposures such as preeclampsia, variation in birth weight, or growth. In contrast, maternal preeclampsia had an impact on cardiac systolic function in addition to that associated with preterm birth.

Increased left ventricular mass index is an independent predictor for cardiovascular morbidity and mortality.<sup>18</sup> The average 19-g-higher left ventricular mass in young adults born preterm is equivalent to that associated with a 9-kg/m<sup>2</sup> increase in body mass index<sup>19</sup> and in longitudinal studies would equate to a >50% increased risk of cardiovascular clinical events in later adult life.<sup>20,21</sup> The major cardiovascular risk previously identified in those born preterm is their higher blood pressure,<sup>9</sup> which could have accounted for a proportion of the increased left ventricular mass. However, we found that, for any given level of blood pressure, prematurity was associated with additional significant increases in left ventricular mass and that the increase in left ventricular mass was graded according to the degree of prematurity independently of other perinatal factors. The presence of increased left ventricular mass in those with hypertension or prehypertension is known to have independent prognostic significance,<sup>21,22</sup> and those born preterm appear to have a disproportionate increase in left ventricular mass relative to their blood pressure.

At birth, there is a change in cardiomyocyte development from fetal to adult arrangement,<sup>3,23</sup> which coincides with an increase in cardiac output and left ventricular end-diastolic pressure.<sup>4,24,25</sup> In preterm birth, this occurs before complete in utero development, and in lambs born preterm, exposure of a relatively immature heart to the sustained increase in afterload and fluctuating preload of postnatal circulation resulted in accelerated cardiomyocyte hypertrophy while the cardiomyocyte number remained static.<sup>2,18</sup> Consistent with this experimental data, Kozák-Bárány et al<sup>23</sup> found that left ventricular mass in humans born preterm increases 56% in the first month postnatally compared with 35% in those born at term. It is possible that the increase in those born preterm merely reflected the expected in utero cardiac growth rate for this point in development. However, our data are consistent with the rapid increase in neonatal left ventricular mass being a pathological event that persists into adult life.

Our decision to use novel computational techniques to build the first atlas of the adult preterm heart provided a valuable tool to capture and analyze 3-dimensional variation in left ventricular geometry in addition to changes in mass. The method we applied was chosen because it allowed, for the first time, the use of a standard 12-slice left ventricular short-axis stack. This meant that some smoothing of the meshes occurred to account for slice gap and shift, but it is potentially more widely clinically applicable than other mesh creation strategies. The atlas analysis avoided specific presuppositions about likely measures of relevance, and we demonstrate that it was powerful enough to identify and quantify variation in a range of geometric factors such as apical position that we would not have captured with standard clinical measures. The

last trimester is important for cardiac growth, and it seems plausible that the short ventricle and reduced cavity size relate to the interruption in development and flow changes seen at preterm birth.<sup>23</sup> Changes in flow patterns within the heart could additionally account for alterations in apical position. However, apical position was also displaced in older adults, suggesting that other factors may be relevant.

Preterm-born lambs have a 5- to 7-fold increase in interstitial, but not perivascular, collagen deposition,<sup>2</sup> characteristic of myocardial pressure overload.<sup>18</sup> The inflammatory cascade of preterm labor has also been proposed to lead to myocardial fibrosis.<sup>26,27</sup> These myocardial patterns would be expected to result in changes in diastolic relaxation, as we observed in the preterm-born young adults.<sup>28</sup> The older adults had similar reductions in diastolic function, and it is possible that there are changes in extracellular matrix, as well as cardiomyocyte appearance and function, within the preterm group, equivalent to changes observed with aging.

In addition to diastolic abnormalities, preterm-born young adults showed unique changes in longitudinal, circumferential, and rotational systolic function.<sup>29</sup> Additionally, maternal preeclampsia was associated with further reductions in left ventricular systolic strain. Preeclampsia is indicative of placental pathology and insufficiency, which may not be a feature of other pregnancies that lead to preterm birth, and offspring of preeclamptic pregnancies develop with reduced uterine perfusion and relative hypoxia from early in gestation.<sup>30</sup> In newborn pigs, short-term exposure to hypoxemia leads to sustained reduction in longitudinal peak systolic strain,<sup>31</sup> thought to result because longitudinal movement is mediated primarily by subendocardial and subepicardial fibers, which are most susceptible to ischemia.<sup>32,33</sup> Although animal models of preeclampsia and pregnancy hypoxia have consistently shown cardiac effects in the offspring, this is the first study in humans to confirm a cardiac-specific impact of preeclampsia.

We were not able to follow up all those initially recruited to the preterm study in the 1980s. Nevertheless, there were no significant differences in demographics or perinatal records between those who took part and the full cohort to suggest that any selection bias was introduced. We can be confident of this because a major strength of the study is the prospective nature of data collection with very detailed information collected at birth. This also allowed us to study the impact of key perinatal factors on later cardiac structure. Previous work has shown that birth weight is a risk factor for coronary heart disease in later life in term-born individuals.<sup>15</sup> It will be of interest to determine whether the hemodynamic changes seen in small-for-gestational-age term-born individuals also lead to cardiac remodeling patterns similar to those we have seen in preterm-born young adults. The study size, although the largest cardiac study of preterm infants, meant that we remained conservative with the number of factors included in our multiple regression analyses. It is likely that other key parameters that may influence left ventricular development will be of interest to investigators and will require subsequent investigation. For example, we have previously investigated the impact of preterm birth on the vasculature,<sup>10,11</sup> and it will be of interest to understand to what extent there is adverse cardiac and

vascular coupling within preterm infants. At present, we also have not addressed whether preterm birth influences right ventricular structure and function or left ventricular radial strain. There are technical challenges in the creation of an accurate 3-dimensional model of the geometrically complex right ventricle, but in due course, we expect to undertake a similar analysis. Reproducibility of radial strain analysis is currently relatively poor,<sup>34</sup> and further development is needed before results can be confidently reported.

## Conclusions

We have demonstrated for the first time that individuals born preterm have a unique left ventricular geometry and function. There is a continuous shift in the demographic of individuals born preterm, with a greater number of younger, smaller preterm-born individuals surviving. Approximately 10% of births are now preterm,<sup>1,35</sup> and with the first generation of very preterm-born survivors now reaching young adulthood, our findings are of considerable public health interest. We believe that understanding whether modifications of these variations in left ventricular structure and function prevent the development of cardiac disease in a growing subgroup of the population will be of interest.

## Sources of Funding

This work was supported by grants to Dr Leeson from the British Heart Foundation (FS/06/024 and FS/11/65/28865). Additional grants were received from the National Institute for Health Research Oxford Biomedical Research Centre, Oxford British Heart Foundation Centre for Research Excellence, and Oxford Health Services Research Committee. A. Lewandowski is supported by the Commonwealth Scholarship Commission. Previous follow-up of this cohort has been supported by the Medical Research Council. The computational atlas work was supported by VPH-Share, European Commission (FP7), contract 269978 (<http://www.vph-share.eu/>).

## Disclosures

None.

## References

1. Beck S, Wojdyla D, Say L, Betran AP, Merialdi M, Requejo JH, Rubens C, Menon R, Look PFV. The worldwide incidence of preterm birth: a systematic review of maternal mortality and morbidity. *Bull World Health Organ*. 2010;88:31–38.
2. Bensley JG, Stacy VK, De Matteo R, Harding R, Black MJ. Cardiac remodelling as a result of pre-term birth: implications for future cardiovascular disease. *Eur Heart J*. 2010;31:2058–2066.
3. Rudolph AM. Myocardial growth before and after birth: clinical implications. *Acta Paediatr*. 2000;89:129–133.
4. Gessner I, Krovetz LJ, Benson RW, Prystowsky H, Stenger V, Eitzman DV. Hemodynamic adaptations in the newborn infant. *Pediatrics*. 1965;36:752–762.
5. Kluckow M. Low systemic blood flow and pathophysiology of the preterm transitional circulation. *Early Hum Dev*. 2005;81:429–437.
6. Karamitsos T, Hudsmith L, Selvanayagam J, Neubauer S, Francis J. Operator induced variability in left ventricular measurements with cardiovascular magnetic resonance is improved after training. *J Cardiovasc Magn Reson*. 2007;9:777–783.
7. Fonseca CG, Backhaus M, Bluemke DA, Britten RD, Chung JD, Cowan BR, Dinov ID, Finn JP, Hunter PJ, Kadish AH, Lee DC, Lima JAC, Medrano-Gracia P, Shivkumar K, Suinesiaputra A, Tao W, Young AA. The Cardiac Atlas Project: an imaging database for computational modeling and statistical atlases of the heart. *Bioinformatics*. 2011;27:2288–2295.
8. Lamata P, Niederer S, Nordsletten D, Barber DC, Roy I, Hose DR, Smith N. An accurate, fast and robust method to generate patient-specific cubic Hermite meshes. *Med Image Anal*. 2011;15:801–813.

9. Lazdam M, de la Horra A, Pitcher A, Mannie Z, Diesch J, Trevitt C, Kyllintreas I, Contractor H, Singhal A, Lucas A, Neubauer S, Kharbanda R, Alp N, Kelly B, Leeson P. Elevated blood pressure in offspring born premature to hypertensive pregnancy: is endothelial dysfunction the underlying vascular mechanism? *Hypertension*. 2010;56:159–165.
10. Lewandowski AJ, Lazdam M, Davis E, Kyllintreas I, Diesch J, Francis J, Neubauer S, Singhal A, Lucas A, Kelly B, Leeson P. Short-term exposure to exogenous lipids in premature infants and long-term changes in aortic and cardiac function. *Arterioscler Thromb Vasc Biol*. 2011;31:2125–2135.
11. Kelly BA, Lewandowski AJ, Worton SA, Davis EF, Lazdam M, Francis J, Neubauer S, Lucas A, Singhal A, Leeson P. Antenatal glucocorticoid exposure and long-term alterations in aortic function and glucose metabolism. *Pediatrics*. 2012;129:e1282–e1290.
12. Lucas A, Morley R, Cole TJ, Gore SM, Lucas PJ, Crowle P, Pearce R, Boon AJ, Powell R. Early diet in preterm babies and developmental status at 18 months. *Lancet*. 1990;335:1477–1481.
13. Lucas A, Morley R, Cole TJ, Lister G, Leeson-Payne C. Breast milk and subsequent intelligence quotient in children born preterm. *Lancet*. 1992;339:261–264.
14. Singhal A, Cole TJ, Fewtrell M, Lucas A. Breastmilk feeding and lipoprotein profile in adolescents born preterm: follow-up of a prospective randomised study. *Lancet*. 2004;363:1571–1578.
15. Leeson CPM, Kattenhorn M, Morley R, Lucas A, Deanfield JE. Impact of low birth weight and cardiovascular risk factors on endothelial function in early adult life. *Circulation*. 2001;103:1264–1268.
16. Gianni D, McKeever S, Yu T, Britten R, Delingette H, Frangi A, Hunter P, Smith N. Sharing and reusing cardiovascular anatomical models over the Web: a step towards the implementation of the virtual physiological human project. *Philos Transact A Math Phys Eng Sci*. 2010;368:3039–3056.
17. Hor KN, Gottlieb WM, Carson C, Wash E, Cnota J, Fleck R, Wansapura J, Klimeczek P, Al-Khalidi HR, Chung ES, Benson DW, Mazur W. Comparison of magnetic resonance feature tracking for strain calculation with harmonic phase imaging analysis. *JACC Cardiovasc Imaging*. 2010;3:144–151.
18. Lorell BH, Carabello BA. Left ventricular hypertrophy: pathogenesis, detection, and prognosis. *Circulation*. 2000;102:470–479.
19. Rider OJ, Lewandowski A, Nethononda R, Petersen SE, Francis JM, Pitcher A, Holloway CJ, Dass S, Banerjee R, Byrne JP, Leeson P, Neubauer S. Gender-specific differences in left ventricular remodelling in obesity: insights from cardiovascular magnetic resonance imaging [published online ahead of print October 10, 2012]. *Eur Heart J*. doi:10.1093/eurheartj/ehs341.
20. Krittayaphong R, Boonyasirinant T, Saiviroonporn P, Thanapiboonpol P, Nakyen S, Ruksakul K, Udompunturak S. Prognostic significance of left ventricular mass by magnetic resonance imaging study in patients with known or suspected coronary artery disease. *J Hypertens*. 2009;27:2249–2256.
21. Levy D, Garrison RJ, Savage DD, Kannel WB, Castelli WP. Prognostic implications of echocardiographically determined left ventricular mass in the Framingham Heart Study. *N Engl J Med*. 1990;322:1561–1566.
22. de Simone G, Verdecchia P, Pedr S, Gorini M, Maggioni AP. Prognosis of inappropriate left ventricular mass in hypertension: the MAVI Study. *Hypertension*. 2002;40:470–476.
23. Kozák-Bárány A, Jokinen E, Saraste M, Tuominen J, Valimäki I. Development of left ventricular systolic and diastolic function in preterm infants during the first month of life: a prospective follow-up study. *J Pediatr*. 2001;139:539–545.
24. Teitel DF, Iwamoto HS, Rudolph AM. Effects of birth-related events on central blood flow patterns. *Pediatr Res*. 1987;22:557–566.
25. St John Sutton M, Gewitz M, Shah B, Cohen A, Reichek N, Gabbe S, Huff D. Quantitative assessment of growth and function of the cardiac chambers in the normal human fetus: a prospective longitudinal echocardiographic study. *Circulation*. 1984;69:645–654.
26. Romero R, Espinoza J, Goncalves LF, Kusanovic JP, Friel LA, Nien JK. Inflammation in preterm and term labour and delivery. *Semin Fetal Neonatal Med*. 2006;11:317–326.
27. Yu Q, Horak K, Larson DF. Role of T lymphocytes in hypertension-induced cardiac extracellular matrix remodeling. *Hypertension*. 2006;48:98–104.
28. Brower GL, Gardner JD, Forman MF, Murray DB, Voloshenyuk T, Levick SP, Janicki JS. The relationship between myocardial extracellular matrix remodeling and ventricular function. *Eur J Cardiothorac Surg*. 2006;30:604–610.
29. Cho G-Y, Marwick TH, Kim H-S, Kim M-K, Hong K-S, Oh D-J. Global 2-dimensional strain as a new prognosticator in patients with heart failure. *J Am Coll Cardiol*. 2009;54:618–624.
30. Davis EF, Newton L, Lewandowski AJ, Lazdam M, Kelly BA, Kyriakou T, Leeson P. Pre-eclampsia and offspring cardiovascular health: mechanistic insights from experimental studies. *Clin Sci (Lond)*. 2012;123:53–72.
31. Borke WB, Edvardsen T, Fugelseth D, Lenes K, Ihlen H, Saugstad OD, Thaulow E. Reduced left ventricular function in hypoxemic newborn pigs: a strain Doppler echocardiographic study. *Pediatr Res*. 2006;59:630–635.
32. Henein MY, Gibson DG. Long axis function in disease. *Heart*. 1999;81:229–231.
33. Jones CJ, Raposo L, Gibson DG. Functional importance of the long axis dynamics of the human left ventricle. *Br Heart J*. 1990;63:215–220.
34. Morton G, Schuster A, Jogiya R, Kutty S, Beerbaum P, Nagel E. Interstudy reproducibility of cardiovascular magnetic resonance myocardial feature tracking. *J Cardiovasc Magn Reson*. 2012;14:43.
35. Martin JA, Hamilton BE, Sutton PD, Ventura SJ, Mathews TJ, Kirmeyer S, Osterman MJ. Births: final data for 2007. *Natl Vital Stat Rep*. 2010;58:1–85.

## CLINICAL PERSPECTIVE

Recent improved survival of infants born prematurely has led to a growing cohort of very preterm infants now entering adulthood. Before birth, these individuals were exposed to a suboptimal intrauterine environment, and after delivery, key developmental stages that would normally occur in utero during the third trimester took place under ex utero physiological conditions. Cardiac development may be particularly affected. Experimental models have demonstrated that after preterm delivery cardiomyocytes undergo accelerated hypertrophy with an increase in interstitial myocardial collagen deposition and that the induced changes are sufficient to remodel the left ventricle. In this study, we used cardiovascular magnetic resonance and a computational atlas to reveal for the first time the impact of preterm birth on left ventricular structure and function in humans. We found that preterm birth is associated with increased left ventricular mass independently of variation in blood pressure and that preterm-born young adults have shorter ventricles, smaller cavity diameters, and a displaced apex compared with term-born control subjects. Furthermore, we have identified distinct changes in left ventricular function related to premature birth, which is significantly worse in those whose mother also had preeclampsia. Because 10% of births are preterm, any adverse health impact of this unusual development pattern is relevant to a large population of adults. Whether interventions to modify these variations in left ventricular structure and function prevent the development of cardiac disease in a growing subgroup of the population will be of future interest.